Squared Sine Adaptive Algorithm and Its Performance Analysis

Xinqi Huang, Yingsong Li, *Senior Member, IEEE,* Yuriy Zakharov, *Senior Member, IEEE,* Yongchun Miao, Zhixiang Huang, *Senior Member, IEEE*, Liping Li

***Abstract*—We presents a squared sine functioned adaptive (SSA) algorithm for acoustic-echo-cancellation (AEC) applications in-presence-of impulsive noise. In the development of the SSA algorithm, a novel cost function is constructed by exerting a sliding window type squared sine function on the estimation error vector, which provides robustness in the impulsive-noise environments and speed-ups convergence when the input is colored signals. Theoretical models for predicting the mean-weight-behavior, transient excess-mean-square-error (EMSE) behavior, and tracking behavior are presented. Moreover, the optimal step size and minimum EMSE of the tracking performance are provided. The computation complexity of SSA algorithm has also been investigated. Numerical experiments demonstrate that the theoretical results match well with simulation results and show the superiority of the proposed SSA algorithm against known algorithms in AEC applications.**

***Index Terms*—AEC, adaptive filters, impulsive-noise, performance analysis.**

I. Introduction

ADAPTIVE filtering (AF) has been widely considered and used for active-noise-control, system identification, beamforming, channel-equalization, acoustic-echo-cancellation (AEC), speech prediction [1], [2]. Among AF algorithms, the least-mean-square (LMS) algorithm [3] is the most often used due to its simple implementation. The LMS utilizes instantaneous squared error to get an error-criterion resulting in its low-complexity, but also a slow convergence. The normalized LMS (NLMS) [4]–[6] is an improved version of LMS to enhance its performance, and it is a variable-step-size algorithm. However, the performance for these LMS-type algorithms will be degraded when the input signals are highly correlated, including speech signal.

To improve the performance, the affine-projection (AP) algorithm and its variants [6]–[10] were created and investigated. The AP-promoted algorithms utilize input signals at previous time and current instants to reduce the colored input influence. At present, these AP-promoted algorithms are mainly discussed and analyzed with a background noise of Gaussian distribution [11], [12]. Nevertheless, the performance of the aforementioned algorithms will degrade when the analyzed signal is contaminated by impulsive noises with heavy-tail distributions.

For improving the convergence of AF algorithms operating in impulsive noises, the AP sign (APS) algorithm [13] has been devised, which minimizes l_1-norm of the *a posteriori* error-vector. The APS does not need matrix inversion, which has low computational-complexity. Additionally, it enhances the convergence in environments with impulsive noise when compared with the original AP algorithm. The AP Versoria (APV) [14] and memory-improved proportionate APS (MIP-APS) [15] algorithms were presented to achieve a faster convergence and lower steady-state misalignment (SSM). The APV algorithm combines data-reuse and Versoria-cost maximization to get a better filter performance. The robust APS (RAPS) algorithm and its shrinking version (SRAPS) are reported in [16]; they minimize a mixed l_1/l_2 norm to speed-ups their convergence speed and significantly reduce the misalignment. Finally, the RAPS and SRAPS algorithms achieve a lower SSM and converge faster than the APS algorithm. However, the algorithms require the matrix inversion, resulting in high computational complexity.

The aforementioned AF algorithms are realized using the mean-squared error (MSE) criterion, constructing from the second-ordered error statistics. Their performances degrade significantly as the probability of large outliers (in the impulsive noise) increases. Recently, the saturation of error nonlinearities, such as in the correntropy concept used against large outliers, has been considered in the literature [17]–[23]. The saturation has been successfully used for developing robust AF algorithms. The maximum-correntropy-criterion (MCC) algorithm with different versions were proposed for applications with background non-Gaussian noise. In addition, variable-kernel-width methods have been used and integrated into the MCC algorithm to balance between SSM and convergence speed using a fixed step-size [21]. Moreover, combining the AP algorithm and generalizing MCC, the AP generalization maximum-correntropy (APGMC) algorithm [24] is constructed to reduce misalignment and enhance the convergence.

The squared sine function obtained from Andrews sine [25] has been investigated in robust statistics, which reveals its effectiveness to recover outliers. For low-power noises or outliers, the squared sine function performs similar to the l_2-norm function, while it behaves similar to the l_1-norm function for high-power noises. Benefiting from its property, the sine estimator is more efficient for trimming outliers described by long-tailed distributions [25], [26]. In this paper, the squared sine adaptive (SSA) algorithm is devised to further enhance the steady-state and convergence performance under

The work of Y. Zakharov was supported in part by the U.K. EPSRC through Grants EP/V009591/1 and EP/R003297/1.

Xinqi Huang is with the College of Information and Communication Engineering, Harbin Engineering University, Harbin 150001, China.

Yingsong Li, Yongchun Miao, Zhixiang Huang and Liping Li are with the Key Laboratory of Intelligent Computing and Signal Processing, Ministry of Education, Anhui University, Hefei 230601, China(e-mail: liyingsong@ieee.org).

Yuriy Zakharov is with the School of Physics, Engineering and Technology, University of York, York YO10 5DD, U.K.

the impulsive environments and correlated signals. Motivated by the AP scheme, the proposed SSA algorithm is realized by taking the gradient-descent-search on a new cost-function obtained from the squared sine function to guarantee robustness against impulsive interferences. Theoretical models for predicting the mean-weight-behavior, transient excess-mean square-error (EMSE) behavior, and tracking behavior of the SSA algorithm are presented and compared with simulation results. Moreover, the optimal step-size and minimum EMSE of tracking behavior of the SSA algorithm are provided. The computational complexity of the SSA algorithm is also investigated. Experimental results validate the correctness of theoretical analysis and show the superiority of the devised SSA algorithm against known algorithms in acoustic echo cancellation applications.

Notations: The scalars, vectors and matrices are marked using normal letters, boldface lowercase letters and boldface uppercase letters. The other related notations are given below.

$(\cdot)^T$ Transpose operation for matrix or vector

$\mathbf{I}$ Identity matrix

$E[\cdot]$ Random variable expectation

$|\cdot|$ Absolute value operator

$\mathrm{Tr}(\cdot)$ Trace of a matrix

II. The Proposed SSA algorithm

For a linear system, the unknown system output is depicted as

$$y(l) = \mathbf{u}^T(l)\mathbf{w}_{\mathrm{o}}, \tag{1}$$

where $\mathbf{w}_{\mathrm{o}} = [w_1, w_2, \cdots, w_{L-1}, w_L]^T$ is the unknown system weight vector and $\mathbf{u}(l)$ is the system input vector of length L. The desired signal is given by

$$d(l) = y(l) + v(l) = \mathbf{u}^T(l)\mathbf{w}_{\mathrm{o}} + v(l), \tag{2}$$

where $v(l)$ is noise in the systems. The estimation-error vector is gotten and written as

$$\mathbf{e}(l) = \mathbf{d}(l) - \mathbf{U}_l^T\mathbf{w}(l). \tag{3}$$

Here, $\mathbf{e}(l) = [e(l), e(l-1), ..., e(l-M+1)]^T$, and $\mathbf{d}(l) = [d(l), d(l-1), ..., d(l-M+1)]^T$, the input matrix is constructed as $\mathbf{U}_l = [\mathbf{u}(l), \mathbf{u}(l-1), ..., \mathbf{u}(l-M+1)]$, M is the projection order, and $\mathbf{w}(l)$ represents an estimate of $\mathbf{w}_{\mathrm{o}}$.

For identification of the unknown system, a new cost function is constructed from the squared sine (obtaining from the Andrews sine [25] function), given by

$$J_{\mathrm{SS}}(l) = \begin{cases} c \cdot \sin^2\left(\frac{e(l)}{2c}\right) & \text{if } |e(l)| \le \pi c \\ c & \text{otherwise} \end{cases}, \tag{4}$$

where c is an adjustable parameter to control the shape of the cost function. The SSA algorithm employs the cost function in (4) to create a data-reuse version, which makes full use of error-information and improves the identification performance in impulsive noise scenarios. Then, a new cost function is created by combining (4) with data-reusing,

$$J_{\mathrm{SSA}}(l) = \sum_{i=0}^{M-1} J_{\mathrm{AS}}(l-i). \tag{5}$$

TABLE I: The SSA algorithm and its computational complexity

Step	Equation	$\times$	$+$	$\sin(\cdot)$
	Initialization: $\mathbf{w}(l) = \mathbf{0}$, for $l \le 0$			$-$
	For $l = 1, 2, 3 \ldots$			$-$
1	$\mathbf{f}(l) = \mathbf{U}^T(l)\,\mathbf{w}(l)$	ML	$M(L-1)$	$-$
2	$\mathbf{e}(l) = \mathbf{d}(l) - \mathbf{f}(l)$	$-$	M	$-$
3	$\mathbf{S}_\mu(l) = \mu \sin(\mathbf{e}(n)/2c)$	$2M$	$-$	M
4	$\mathbf{w}(l+1) = \mathbf{w}(l) + \mathbf{U}_l\mathbf{S}_\mu(l)$	ML	ML	$-$
Totail: $2ML + 2M$ multiplications, $2ML$ additions, M sine operations.				

Taking partial-derivative in (5) in relation to $\mathbf{w}(l)$, we get

$$\begin{aligned} \frac{\partial J_{\mathrm{SSA}}(l)}{\partial \mathbf{w}(l)} &= \frac{\partial}{\partial \mathbf{w}(l)} \sum_{i=0}^{M-1} 2c \cdot \sin^2\left(\frac{e(l-i)}{2c}\right) \\ &= -\sum_{i=0}^{M-1} \sin\left(\frac{e(l-i)}{2c}\right)\mathbf{u}(l-i) \\ &= -\mathbf{U}_l \sin\left(\frac{\mathbf{e}(l)}{2c}\right), \end{aligned} \tag{6}$$

when $|e(l-i)| \le \pi c, i = 0, 1, \ldots, M-1$. If $|e(l-i)| > \pi c$, the value of $\partial J_{\mathrm{AS}}(l)/\partial \mathbf{w}(l)$ is equal to zero.

Using the gradient-descent-method [27], the SSA weight update-equation is defined as

$$\mathbf{w}(l+1) = \mathbf{w}(l) - \mu \frac{\partial}{\partial \mathbf{w}(l)} J_{\mathrm{SSA}}(l), \tag{7}$$

where μ is a step-size, which is chosen to offer a tradeoff between the convergence-rate and misalignment. From eqs. (6) and (7), we have

$$\mathbf{w}(l+1) = \mathbf{w}(l) + \mu \mathbf{U}_l \sin\left(\frac{\mathbf{e}(l)}{2c}\right), \tag{8}$$

while $e(l-i)$ is set to zero when $|e(l-i)| > \pi c$. For large values of $e(l-i)$, the weight update is a small value and thus the SSA algorithm achieves stable performance in the presence of outliers.

The implementating complexity of devised SSA algorithm is briefly discussed in Table I. Steps 1 and 4 have the most computations and we use a look-up table for the $\sin(\cdot)$ to reduce the complexity of non-linear operations. Table II is a comparisons of multiplications, additions, and divisions for recent reported APS, AP, APV, and SSA algorithms for each iteration. The AP algorithm gives the highest computation burdens as it uses matrix inversion, while SSA algorithm is simpler compared to these popular AP-like algorithms.

TABLE II: Complexities of the SSA and recent AP-like AF algorithm.

Algorithm	Multiplication	Division	Addition
AP	$(M^2+2M)L+M^3+M$	$-$	$(M^2+2M)L+M^3+M^2-M$
APS	$2ML+M^2+4M$	1	$2ML+M^2+2M-1$
APV	$ML+L+2M^2+6M+2$	$M+1$	$ML+L+2M^2+4M$
SSA	$2ML+2M$	$-$	$2ML$

III. The mean weight analysis

Theoretical analysis for SSA algorithm is now carried out to obtain its transient mean weight (MW) behavior. The MW analysis can indicate the instantaneous behavior of the weight vector. Let $\tilde{\mathbf{w}}(l) = \mathbf{w}(l) - \mathbf{w}_{\mathrm{o}}$, then (3) is rewritten as

$$\begin{aligned} \mathbf{e}(l) &= \mathbf{v}(l) - \mathbf{e}_a(l) \\ &= \mathbf{v}(l) - \mathbf{U}_l^T\tilde{\mathbf{w}}(l), \end{aligned} \tag{9}$$

where $\mathbf{e}_a(l)$ is *a priori* error vector. Then, the weighting update-equation is

$$\begin{aligned}\tilde{\mathbf{w}}(l+1) &= \mathbf{w}(l+1) - \mathbf{w}_{\mathrm{o}} \\ &= \mu \mathbf{U}_l \sin\left(\frac{\mathbf{e}(l)}{2c}\right) + \tilde{\mathbf{w}}(n).\end{aligned} \tag{10}$$

Taking expectation in (10), we get

$$\begin{aligned}E[\tilde{\mathbf{w}}(l+1)] &= E[\tilde{\mathbf{w}}(l)] + \mu E\left[\mathbf{U}_l \sin\left(\frac{\mathbf{e}(l)}{2c}\right)\right] \\ &= E[\tilde{\mathbf{w}}(l)] + \mu \sum_{i=0}^{M-1} E\left[\mathbf{u}(l-i)\sin\left(\frac{e(l-i)}{2c}\right)\right].\end{aligned} \tag{11}$$

To analyze the nonlinearity terms $\sin(e(l-i)/2c), i = 0, 1, \ldots, M-1$, several assumptions are normally considered in the convergence analysis [28]–[31].

Assumption 1: $v(l)$ are zero mean (ZM) and i.i.d. variables, independent of other signal.

Assumption 2: $\tilde{\mathbf{w}}(l)$ is independent of other signal.

Assumption 3: The input $\mathbf{u}(l)$ is i.i.d. signal with covariance matrix $\mathbf{R}_u(\tau) = E[\mathbf{u}(l)\mathbf{u}^T(l+\tau)]$, where τ indicates a delay between the input vectors.

Taking the Taylor-series expansion of $\sin(e(l-i)/2c)$ in relation to $e_a(l-i)$ at $v(l-i)$, yields

$$\begin{aligned}\sin\left(\frac{e(l-i)}{2c}\right) &= \sin\left(\frac{v(l-i)-e_a(l-i)}{2c}\right) \\ &= \sin\left(\frac{v(l-i)}{2c}\right) - \frac{\cos\left(\frac{v(l-i)}{2c}\right)e_a(l-i)}{2c} \\ &- \frac{\sin\left(\frac{v(l-i)}{2c}\right)e_a^2(l-i)}{c^2} + o\left(e_a^2(l-i)\right),\end{aligned} \tag{12}$$

where $o\left(e_a^2(l-i)\right)$ refers to the third and higher-order terms. If $o\left(e_a^2(l-i)\right)$ is small enough, then based on the Assumptions 1, 2, and 3, we obtain

$$\begin{aligned}E\left[\mathbf{u}(l-i)\sin\left(\frac{e(l-i)}{2c}\right)\right] &\approx -E\left[\frac{\cos\left(\frac{v(l-i)}{2c}\right)\mathbf{u}(l-i)e_a(l-i)}{2c}\right] \\ &= -E\left[\frac{\cos\left(\frac{v(l-i)}{2c}\right)\mathbf{u}(l-i)\mathbf{u}^T(l-i)\tilde{\mathbf{w}}(l)}{2c}\right] \\ &= -\frac{1}{2c}E\left[\cos\left(\frac{v(l)}{2c}\right)\right]\mathbf{R}_u(0)E[\tilde{\mathbf{w}}(l)],\end{aligned} \tag{13}$$

where $E[\sin(v(l)/2c)] = 0$ because of Assumption 1. The value of $\sin(v(l)/2c)$ is set to zero when $|v(l)| > \pi c$. Thus, we obtain the MW recursion in the SSA algorithm as

$$E[\tilde{\mathbf{w}}(l+1)] = E[\tilde{\mathbf{w}}(l)] - \mu\frac{M}{2c}E\left[\cos\left(\frac{v(l)}{2c}\right)\right]\mathbf{R}_u(0)E[\tilde{\mathbf{w}}(l)]. \tag{14}$$

The simulation results reported in section VI illustrate the model accuracy.

IV. The transient EMSE analysis

Transient EMSE is a widely-used measure for evaluating convergence performance of AF-algorithms [28]–[30]. Using Assumptions 2 and 3, the transient EMSE can be obtained from

$$\mathrm{T_{EMSE}} = E\left[\left(\mathbf{u}^T(l)\tilde{\mathbf{w}}(l)\right)^2\right] \approx \mathrm{trace}\left[\mathbf{A}_{\tilde{\mathbf{w}}}(l)\mathbf{R}_u(0)\right], \tag{15}$$

where $\mathbf{A}_{\tilde{\mathbf{w}}}(l) = E\left[\tilde{\mathbf{w}}(l)\tilde{\mathbf{w}}^T(l)\right]$. From equation (15), the recursion model of $\mathbf{A}_{\tilde{\mathbf{w}}}(l) = E\left[\tilde{\mathbf{w}}(l)\tilde{\mathbf{w}}^T(l)\right]$ is the key to obtain the transient EMSE by using equation (10).

Multiplying (10) by its transpose yields

$$\begin{aligned}\tilde{\mathbf{w}}(l+1)\tilde{\mathbf{w}}^T(l+1) &= \tilde{\mathbf{w}}(l)\tilde{\mathbf{w}}^T(l) + \mu\tilde{\mathbf{w}}(l)\sin\left(\frac{\mathbf{e}^T(l)}{2c}\right)\mathbf{U}_l^T \\ &+ \mu\mathbf{U}_l\sin\left(\frac{\mathbf{e}(l)}{2c}\right)\tilde{\mathbf{w}}^T(l) + \mu^2\mathbf{U}_l\sin\left(\frac{\mathbf{e}(l)}{2c}\right)\sin\left(\frac{\mathbf{e}^T(l)}{2c}\right)\mathbf{U}_l^T.\end{aligned} \tag{16}$$

Therefore, taking expectations on (16), yields

$$\begin{aligned}\mathbf{A}_{\tilde{\mathbf{w}}}(l+1) &= \mathbf{A}_{\tilde{\mathbf{w}}}(l) + \mu E\left[\tilde{\mathbf{w}}(l)\sin\left(\frac{\mathbf{e}^T(l)}{2c}\right)\mathbf{U}_l^T\right] \\ &+ \mu E\left[\mathbf{U}_l\sin\left(\frac{\mathbf{e}(l)}{2c}\right)\tilde{\mathbf{w}}^T(l)\right] + \mu^2 E\left[\mathbf{U}_l\sin\left(\frac{\mathbf{e}(l)}{2c}\right)\sin\left(\frac{\mathbf{e}^T(l)}{2c}\right)\mathbf{U}_l^T\right].\end{aligned} \tag{17}$$

We have

$$E\left[\mathbf{U}_l\sin\left(\frac{\mathbf{e}(l)}{2c}\right)\tilde{\mathbf{w}}^T(l)\right] = \sum_{i=0}^{M-1} E\left[\mathbf{u}(l-i)\sin\left(\frac{e(l-i)}{2c}\right)\tilde{\mathbf{w}}^T(l)\right]. \tag{18}$$

Substituting (12) into (18), we obtain

$$\begin{aligned}&E\left[\mathbf{u}(l-i)\sin\left(\frac{e(l-i)}{2c}\right)\tilde{\mathbf{w}}^T(l)\right] \\ &\approx E\left[\sin\left(\frac{v(l-i)}{2c}\right)\mathbf{u}(l-i)\tilde{\mathbf{w}}^T(l)\right] \\ &- E\left[\frac{\cos\left(\frac{v(l-i)}{2c}\right)\mathbf{u}(l-i)e_a(l-i)\tilde{\mathbf{w}}^T(l)}{2c}\right] \\ &- E\left[\frac{\sin\left(\frac{v(l-i)}{2c}\right)e_a^2(l-i)\mathbf{u}(l-i)\tilde{\mathbf{w}}^T(l)}{8c^2}\right] \\ &\approx -E\left[\frac{\cos\left(\frac{v(l-i)}{2c}\right)\mathbf{u}(l-i)\mathbf{u}^T(l-i)\tilde{\mathbf{w}}(l)\tilde{\mathbf{w}}^T(l)}{2c}\right] \\ &= -\frac{1}{2c}E\left[\cos\left(\frac{v(l)}{2c}\right)\right]\mathbf{R}_u(0)\mathbf{A}_{\tilde{\mathbf{w}}}(l).\end{aligned} \tag{19}$$

Then, (18) changes to

$$E\left[\mathbf{U}_l\sin\left(\frac{\mathbf{e}(l)}{2c}\right)\tilde{\mathbf{w}}^T(l)\right] \approx -\frac{M}{2c}E\left[\cos\left(\frac{v(l)}{2c}\right)\right]\mathbf{R}_u(0)\mathbf{A}_{\tilde{\mathbf{w}}}(l). \tag{20}$$

Using the same approach, we obtain

$$E\left[\tilde{\mathbf{w}}(l)\sin\left(\frac{\mathbf{e}^T(l)}{2c}\right)\mathbf{U}_l^T\right] \approx -\frac{M}{2c}E\left[\cos\left(\frac{v(l)}{2c}\right)\right]\mathbf{A}_{\tilde{\mathbf{w}}}(l)\mathbf{R}_u(0). \tag{21}$$

Assume that $\sin\left(\frac{e(l)}{2c}\right) \approx \sin\left(\frac{e(l-1)}{2c}\right) \approx \cdots \approx \sin\left(\frac{e(l-M+1)}{2c}\right)$ which is valid in the steady state of the SSA algorithm. Then, utilizing same method for getting the term $E\left[\mathbf{U}_l\sin\left(\frac{\mathbf{e}(l)}{2c}\right)\sin\left(\frac{\mathbf{e}^T(l)}{2c}\right)\mathbf{U}_l^T\right]$, yields

$$E\left[\mathbf{U}_l\sin\left(\frac{\mathbf{e}(l)}{2c}\right)\sin\left(\frac{\mathbf{e}^T(l)}{2c}\right)\mathbf{U}_l^T\right] \approx E\left[\sin^2\left(\frac{e(l)}{2c}\right)\mathbf{U}_l\mathbf{1}\mathbf{1}^T\mathbf{U}_l^T\right], \tag{22}$$

where $\mathbf{1}^T = [1, 1, \ldots, 1]$ is a vector of ones of length M. Taking Taylor-expansion of $\sin^2\left(\frac{e(l)}{2c}\right)$ in terms of $e_a(l)$

around $v(l)$, we get

$$\sin^2\!\left(\frac{e(l)}{2c}\right)=\sin^2\left(\frac{v(l)}{2c}\right)-\frac{\cos\left(\frac{v(l)}{2c}\right)\sin\left(\frac{v(l)}{2c}\right)e_a(l)}{c} - \frac{\left(\sin^2\left(\frac{v(l)}{2c}\right)-\cos^2\left(\frac{v(l)}{2c}\right)\right)e_a^2(l)}{4c^2}+o\left(e_a^2(l)\right). \tag{23}$$

Then, we get

$$\begin{aligned} &E\left[\mathbf{U}_l\sin\left(\frac{\mathbf{e}(l)}{2c}\right)\sin\left(\frac{\mathbf{e}^T(l)}{2c}\right)\mathbf{U}_l^T\right]\\ &\approx E\left[\sin^2\left(\frac{v(l)}{2c}\right)\mathbf{U}_l\mathbf{1}\mathbf{1}^T\mathbf{U}_l^T\right]\\ &-\frac{1}{c}E\left[\sin\left(\frac{v(l)}{2c}\right)\cos\left(\frac{v(l)}{2c}\right)e_a(l)\,\mathbf{U}_l\mathbf{1}\mathbf{1}^T\mathbf{U}_l^T\right]\\ &-\frac{1}{4c^2}E\left[\left(\sin^2\left(\frac{v(l)}{2c}\right)-\cos^2\left(\frac{v(l)}{2c}\right)\right)e_a^2(l)\,\mathbf{U}_l\mathbf{1}\mathbf{1}^T\mathbf{U}_l^T\right]\\ &=E\left[\sin^2\left(\frac{v(l)}{2c}\right)\mathbf{U}_l\mathbf{1}\mathbf{1}^T\mathbf{U}_l^T\right]\\ &-\frac{1}{4c^2}E\left[\left(\sin^2\left(\frac{v(l)}{2c}\right)-\cos^2\left(\frac{v(l)}{2c}\right)\right)e_a^2(l)\,\mathbf{U}_l\mathbf{1}\mathbf{1}^T\mathbf{U}_l^T\right]. \end{aligned} \tag{24}$$

The last term in (24) can be rewritten as

$$\begin{aligned} &\frac{1}{4c^2}E\left[\left(\sin^2\left(\frac{v(l)}{2c}\right)-\cos^2\left(\frac{v(l)}{2c}\right)\right)e_a^2(l)\,\mathbf{U}_l\mathbf{1}\mathbf{1}^T\mathbf{U}_l^T\right]\\ &=\frac{1}{4c^2}E\left[\sin^2\left(\frac{v(l)}{2c}\right)-\cos^2\left(\frac{v(l)}{2c}\right)\right]\\ &\times E\left\{\left[\sum_{i=0}^{M-1}\mathbf{u}(l-i)\right]\mathbf{u}^T(l)\tilde{\mathbf{w}}(l)\tilde{\mathbf{w}}^T(l)\mathbf{u}(l)\left[\sum_{i=0}^{M-1}\mathbf{u}^T(l-i)\right]\right\}\\ &\approx\frac{1}{4c^2}E_{sc2}\mathbf{R}_u^M\mathbf{A}_{\tilde{\mathbf{w}}}(l)\,\mathbf{R}_u^M, \end{aligned} \tag{25}$$

where $\mathbf{R}_u^M=\mathbf{R}_u(0)+\mathbf{R}_u(1)+\cdots+\mathbf{R}_u(M-1)$ and $E_{sc2}=E\left[\sin^2\left(\frac{v(l)}{2c}\right)-\cos^2\left(\frac{v(l)}{2c}\right)\right]$. Substituting (25) into (24), yields

$$\begin{aligned} E\left[\mathbf{U}_l\sin\left(\frac{\mathbf{e}(l)}{2c}\right)\sin\left(\frac{\mathbf{e}^T(l)}{2c}\right)\mathbf{U}_l^T\right]&\approx E\left[\sin^2\left(\frac{v(l)}{2c}\right)\right]E\left[\mathbf{U}_l\mathbf{1}\mathbf{1}^T\mathbf{U}_l^T\right]\\ &-\frac{1}{4c^2}E_{sc2}\mathbf{R}_u^M\mathbf{A}_{\tilde{\mathbf{w}}}(l)\,\mathbf{R}_u^M. \end{aligned} \tag{26}$$

Furthermore, substituting (20), (21) and (26) into (17), the recursion for $\mathbf{A}_{\tilde{\mathbf{w}}}(l)$ can be obtained, given by

$$\begin{aligned} \mathbf{A}_{\tilde{\mathbf{w}}}(l+1)&=\mathbf{A}_{\tilde{\mathbf{w}}}(l)-\mu\frac{M}{2c}E\left[\cos\left(\frac{v(l)}{2c}\right)\right]\mathbf{A}_{\tilde{\mathbf{w}}}(l)\,\mathbf{R}_u(0)\\ &-\mu\frac{M}{2c}E\left[\cos\left(\frac{v(l)}{2c}\right)\right]\mathbf{R}_u(0)\,\mathbf{A}_{\tilde{\mathbf{w}}}(l)\\ &+\mu^2E\left[\sin^2\left(\frac{v(l)}{2c}\right)\right]E\left[\mathbf{U}_l\mathbf{1}\mathbf{1}^T\mathbf{U}_l^T\right]\\ &-\frac{\mu^2}{4c^2}E_{sc2}\mathbf{R}_u^M\mathbf{A}_{\tilde{\mathbf{w}}}(l)\,\mathbf{R}_u^M. \end{aligned} \tag{27}$$

The simulating results obtained in Section VI helps to verify an excellent accuracy of the theoretical prediction.

V. Tracking analysis

In this section, the behavior of SSA algorithm is assessed in non-stationary environment. We assume that $\mathbf{w}_o(l)$ is time-varying referring to random walk model [10],

$$\mathbf{w}_o(l+1)=\mathbf{w}_o(l)+\mathbf{h}(l), \tag{28}$$

where $\mathbf{h}(l)$ is an i.i.d. ZM Gaussian sequence of vectors with the auto-correlation matrix $\mathbf{Q}=E\left[\mathbf{h}(l)\,\mathbf{h}^T(l)\right]=\sigma_h^2\mathbf{I}_L$.

Substituting (28) into (10), we have

$$\tilde{\mathbf{w}}(l+1)=\tilde{\mathbf{w}}(l)+\mu\mathbf{U}_l\sin\left(\frac{\mathbf{e}(l)}{2c}\right)-\mathbf{h}(l). \tag{29}$$

Left multiplying $\mathbf{U}_l^T$ on (29), we obtain

$$\tilde{\mathbf{e}}_p(l)=\tilde{\mathbf{e}}(l)+\mu\mathbf{U}_l^T\mathbf{U}_l\sin\left(\frac{\mathbf{e}(l)}{2c}\right) \tag{30}$$

with

$$\tilde{\mathbf{e}}(l)\triangleq\mathbf{U}_l^T\tilde{\mathbf{w}}(l)=\mathbf{v}(l)-\mathbf{e}(l), \tag{31}$$

$$\begin{aligned} \tilde{\mathbf{e}}_p(l)&\triangleq\mathbf{U}_l^T\left(\tilde{\mathbf{w}}(l+1)+\mathbf{h}(l)\right)\\ &=\mathbf{U}_l^T\left(\mathbf{w}(l+1)-\mathbf{w}_o(l)\right). \end{aligned} \tag{32}$$

Using (29) and (30), following relation is gotten between estimation errors

$$\tilde{\mathbf{w}}(l+1)=\tilde{\mathbf{w}}(l)+\mathbf{U}_l\left(\mathbf{U}_l^T\mathbf{U}_l\right)^{-1}\left(\tilde{\mathbf{e}}_p(l)-\tilde{\mathbf{e}}(l)\right)-\mathbf{h}(l). \tag{33}$$

Taking the square of the l_2-norm and expectations on (33), we obtain

$$\begin{aligned} &E\left[\|\tilde{\mathbf{w}}(l+1)+\mathbf{h}(l)\|_2^2\right]+E\left[\tilde{\mathbf{e}}^T(l)\left(\mathbf{U}_l^T\mathbf{U}_l\right)^{-1}\tilde{\mathbf{e}}(l)\right]\\ &=E\left[\|\tilde{\mathbf{w}}(l)\|_2^2\right]+E\left[\tilde{\mathbf{e}}_p^T(l)\left(\mathbf{U}_l^T\mathbf{U}_l\right)^{-1}\tilde{\mathbf{e}}_p(l)\right]. \end{aligned} \tag{34}$$

Substituting (30) and (29) into (33), the equation (34) can be rewritten as

$$\begin{aligned} E\left[\|\tilde{\mathbf{w}}(l+1)\|^2\right]&=E\left[\|\tilde{\mathbf{w}}(l)\|^2\right]+2\mu E\left[\mathbf{e}_a^T(l)\sin\left(\frac{\mathbf{e}(l)}{2c}\right)\right]\\ &+\mu^2E\left[\sin\left(\frac{\mathbf{e}^T(l)}{2c}\right)\mathbf{U}_l^T\mathbf{U}_l\sin\left(\frac{\mathbf{e}(l)}{2c}\right)\right]+\mathrm{Tr}(\mathbf{Q}). \end{aligned} \tag{35}$$

Assuming that weight error-vector reaches a steady-state-mean-squared value, yields

$$\lim_{l\to\infty}E\left[\|\tilde{\mathbf{w}}(l+1)\|^2\right]=\lim_{l\to\infty}E\left[\|\tilde{\mathbf{w}}(l)\|^2\right]. \tag{36}$$

From (35) we have

$$\begin{aligned} \lim_{n\to\infty}\mu E\left[\sin\left(\frac{\mathbf{e}^T(l)}{2c}\right)\mathbf{U}_l^T\mathbf{U}_l\sin\left(\frac{\mathbf{e}(l)}{2c}\right)\right]+\mathrm{Tr}(\mathbf{Q})&=\\ -2\lim_{n\to\infty}E\left[\mathbf{e}_a(l)\sin\left(\frac{\mathbf{e}(l)}{2c}\right)\right]. \end{aligned} \tag{37}$$

Then, right-hand side of (37) changes to

$$\lim_{l\to\infty}E\left[\mathbf{e}_a^T(l)\sin\left(\frac{\mathbf{e}(l)}{2c}\right)\right]\approx M\lim_{l\to\infty}E\left[e_a(l)\sin\left(\frac{e(l)}{2c}\right)\right]. \tag{38}$$

Combining (12) and (38), we obtain

$$\begin{aligned} \lim_{l\to\infty}E\left[\mathbf{e}_a^T(l)\sin\left(\frac{\mathbf{e}(l)}{2c}\right)\right]&=-\frac{M}{2c}E\left[\cos\left(\frac{v(l)}{2c}\right)\right]\lim_{l\to\infty}E\left[e_a^2(l)\right]\\ &=-\frac{M}{2c}E\left[\cos\left(\frac{v(l)}{2c}\right)\right]\mathrm{EMSE}, \end{aligned} \tag{39}$$

where $\mathrm{EMSE}\triangleq\lim_{l\to\infty}E\left[e_a^2(l)\right]$. Similarly to the derivation of

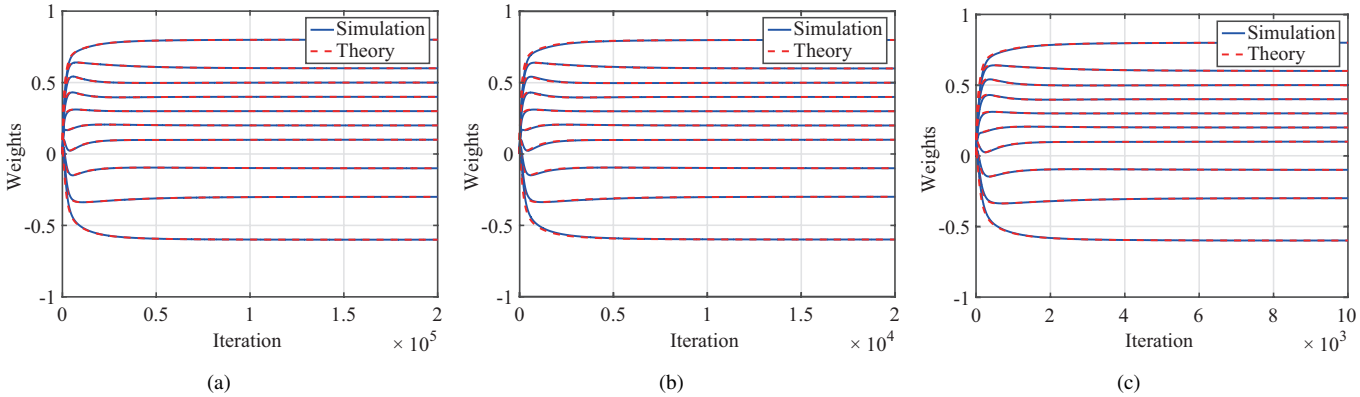

Fig. 1: Weight performance of the SSA with different M and $P = 0.001$. (a) $M = 1$; (b) $M = 8$; (c) $M = 16$.

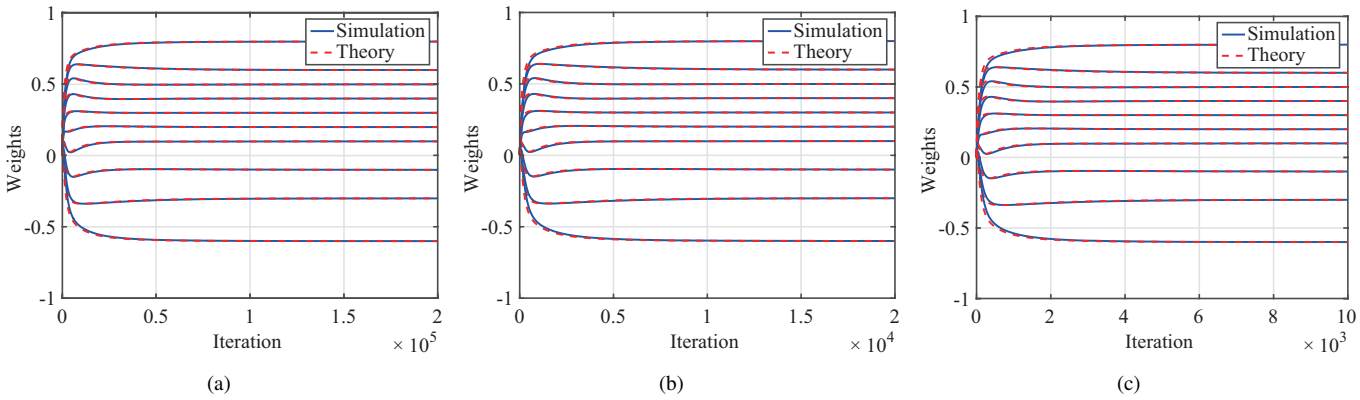

Fig. 2: Weight performance of the SSA with different M and $P = 0.1$. (a) $M = 1$; (b) $M = 8$; (c) $M = 16$.

(22), the left-hand side of (37) is rewritten as

$$\begin{aligned}\lim_{l\to\infty} E\left[\sin\left(\frac{\mathbf{e}^T(l)}{2c}\right)\mathbf{U}_l^T\mathbf{U}_l\sin\left(\frac{\mathbf{e}(l)}{2c}\right)\right] &= E\left[\mathbf{1}^T\mathbf{U}_l^T\mathbf{U}_l\mathbf{1}\right]\lim_{l\to\infty} E\left[\sin^2\left(\frac{e(l)}{2c}\right)\right] \\ &\approx E\left[\mathbf{1}^T\mathbf{U}_l^T\mathbf{U}_l\mathbf{1}\right]E\left[\sin^2\left(\frac{v(l)}{2c}\right)\right] \\ &\quad -\frac{1}{4c^2}E\left[\mathbf{1}^T\mathbf{U}_l^T\mathbf{U}_l\mathbf{1}\right]\mathrm{EMSE} \\ &= S_u E\left[\sin^2\left(\frac{v(l)}{2c}\right)\right] \\ &\quad -\frac{S_u}{4c^2}E_{sc2}\mathrm{EMSE},\end{aligned} \tag{40}$$

where $S_u \triangleq E\left[\mathbf{1}^T\mathbf{U}_l^T\mathbf{U}_l\mathbf{1}\right]$. Substituting (39) and (40) into (37) yields

$$\begin{aligned}\mu S_u E\left[\sin^2\left(\frac{v(l)}{2c}\right)\right] - \frac{\mu}{4c^2}S_u E_{sc2}\mathrm{EMSE} + \mathrm{Tr}(\mathbf{Q}) \\ = \frac{M}{c}E\left[\cos\left(\frac{v(l)}{2c}\right)\right]\mathrm{EMSE}.\end{aligned} \tag{41}$$

After some algebra, we can obtain

$$\begin{aligned}\mathrm{EMSE} &= \frac{4c^2\mu^2 S_u E\left[\sin^2\left(\frac{v(l)}{2c}\right)\right] + 4c^2 L\sigma_h^2}{4c\mu M E\left[\cos\left(\frac{v(l)}{2c}\right)\right] + \mu^2 S_u E_{sc2}} \\ &= \frac{4c^2\mu^2 S_u E_{s2} + 4c^2 L\sigma_h^2}{4c\mu M E_{c1} + \mu^2 S_u E_{sc2}},\end{aligned} \tag{42}$$

where $E_{s2} \triangleq E\left[\sin^2\left(\frac{v(l)}{2c}\right)\right]$ and $E_{c1} \triangleq E\left[\cos\left(\frac{v(l)}{2c}\right)\right]$.

Taking the derivative of (42) with respect to μ, yields

$$\begin{aligned}\mathrm{EMSE}' = &\left(\frac{1}{E_{sc}^2 S_u^2\mu^4 + 8E_{c1}E_{sc}MS_u c\mu^3 + 16E_{c1}^2M^2c^2\mu^2}\right) \\ &\times\left(16E_{s2}E_{c1}MS_u c^3\mu^2 - 8E_{sc}LS_u c^2\sigma_h^2\mu - 16E_{c1}LMc^3\sigma_h^2\right).\end{aligned} \tag{43}$$

Making (43) equal to zero, the optimized μ for minimizing EMSE is obtained as

$$\mu_o = \frac{\sqrt{E_{sc}^2L^2\sigma_h^4S_u^2 + 16c^2M^2L\sigma_h^2S_u E_{s2}E_{c1}^2} + L\sigma_h^2S_uE_{sc}}{4cMS_uE_{s2}E_{c1}}, \tag{44}$$

and the minimum EMSE is given by

$$\mathrm{EMSE}_{\min} = \frac{4c^2\mu_o^2S_uE_{s2} + 4c^2L\sigma_h^2}{4c\mu_oME_{c1} + \mu_o^2S_uE_{sc}}. \tag{45}$$

VI. Simulation Results

To show the effectiveness of devised SSA and the correctness of theoretical analysis, experiments are set up and investigated. Results in all experiments are derived from averaging over 500 independent Monte-Carlo trials. $v(l)$ is added to system output with $v(l) = b(l) + \eta(l)q(l)$ [25], where $\eta(l)$ is i.i.d. Bernoulli-random sequence in which occurrence probability $\Pr[\eta(l) = 1] = P$ and $\Pr[\eta(l) = 0] = 1 - P$. The sequences $b(l)$ and $q(l)$ are i.i.d. ZM white Gaussian noises (WGNs), and their variances are σ_b^2 and σ_q^2 ($\sigma_q^2 \gg \sigma_b^2$), respectively. The mean-squared deviation (MSD) is adopted in the simulations, defined as $\mathrm{NMSD}(l) = 10\log_{10}\left[\|\mathbf{w}(l) - \mathbf{w}_o\|^2/\|\mathbf{w}_o\|^2\right]$ to measure identification

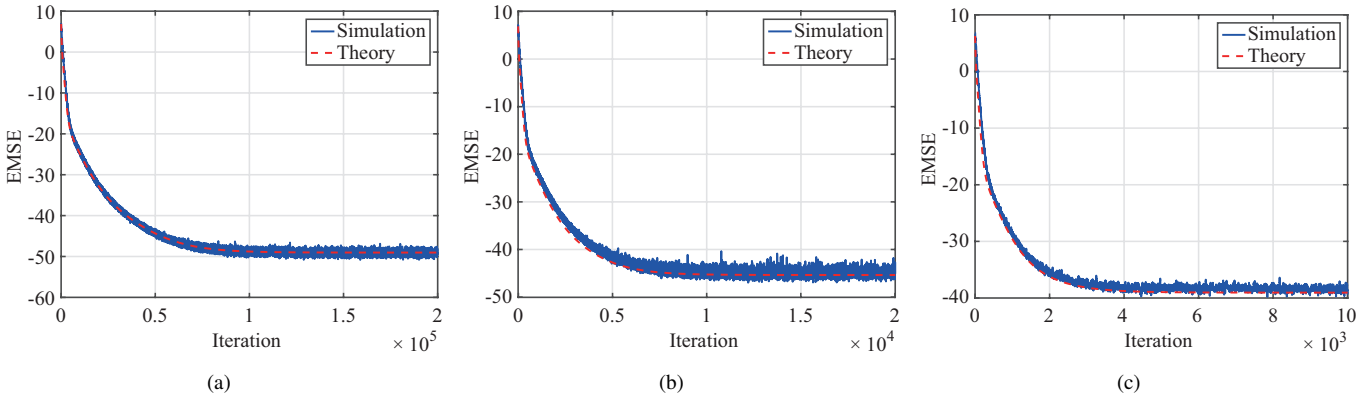

Fig. 3: Transient performance of the SSA with M and $P = 0.001$. (a) $M = 1$; (b) $M = 8$; (c) $M = 16$.

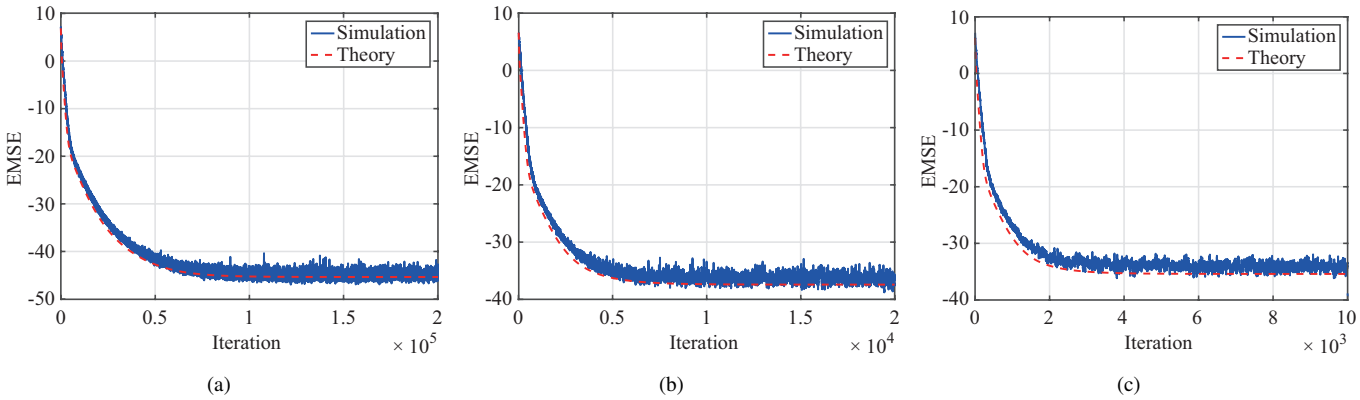

Fig. 4: Transient performance of the SSA with different M and $P = 0.1$. (a) $M = 1$; (b) $M = 8$; (c) $M = 16$.

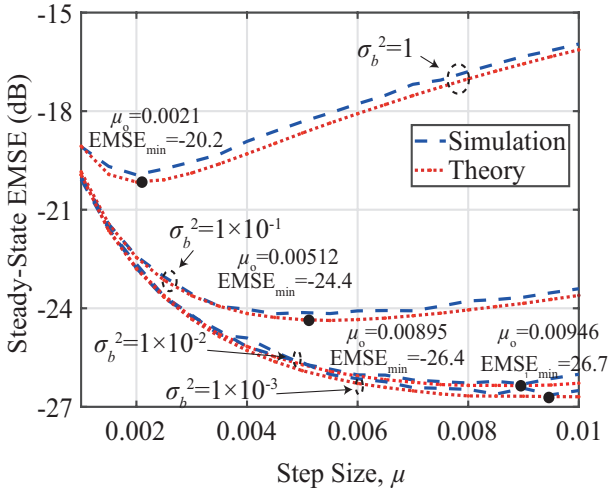

Fig. 5: Steady state EMSE for $\sigma_h^2 = 1 \times 10^{-6}$ vs. μ for variousσ_b^2.

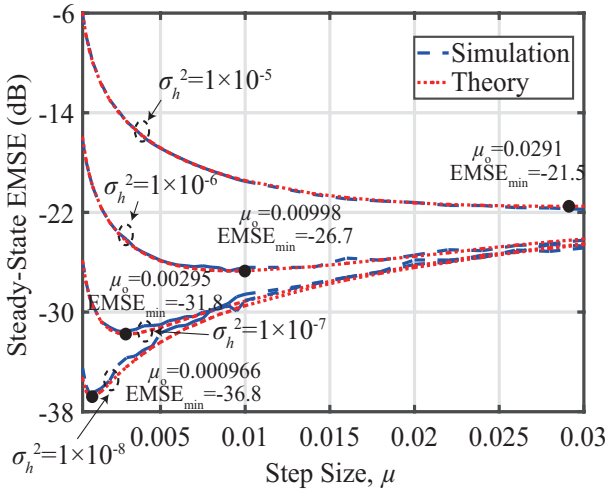

Fig. 6: Steady state EMSE with $\sigma_b^2 = 1 \times 10^{-3}$ vs. μ for various σ_h^2.

performance of the algorithm,where initial weight-vectors are zero.

A. Evaluation of Mean Weight

The mean weight results are investigated in the following scenario. The input signal is a first-order auto-regression (AR) process that has correlation-coefficient of 0.9. The unknown system is considered to have the weight vector $\mathbf{w}_o = [0.8, 0.6, 0.5, 0.4, 0.3, 0.2, 0.1 - 0.1 - 0.3 - 0.6]^T$ as in [32]. The impulsive-noise $v(n)$ is put into system to get a SN) of 30 dB and a signal-to-interference ratio (SIR) of -30 dB, where SNR is $\mathrm{SNR} = 10\log_{10}\left\{E\left[\mathrm{y}^2(l)\right]/\sigma_b^2\right\}$ and SIR is $\mathrm{SIR}=10\log_{10}\left\{E\left[\mathrm{y}^2(l)\right]/\sigma_q^2\right\}$.

Figs. 1 and 2 show the MW curves for different values of M with $P = 0.1$ and $P = 0.001$. The parameters in these experiments are $\mu = 0.001$ and $c = 1$. Figs. 1 and 2 illustrate a very good agreement of the theoretical analysis with the corresponding simulation results, which demonstrate the accuracy of the analysis.

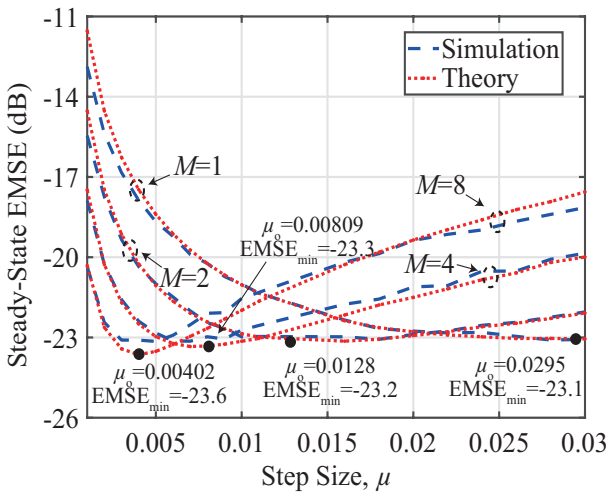

Fig. 7: Steady state EMSE against μ with different M and $\sigma_s^2 = 1 \times 10^{-3}$, $\sigma_h^2 = 1 \times 10^{-6}$.

B. Evaluation of Transient EMSE

The transient EMSE is now investigated via simulation experiments. The parameters of these experiments are the same as in the MW experiments. Figs. 3 and 4 show the theoretical transient curves for different values of M with $P = 0.001$ and $P = 0.1$, respectively. The theoretical results predict well the performance of SSA algorithm, which shows that although we made an approximation in Equation (21), the results from the simulations verify the theoretical analysis accuracy.

C. Evaluation of Tracking EMSE

The theoretical analysis of the tracking performance is now verified by experiments. The system and input signal are same. The occurrence probability is set to $P = 0.005$ [14]. The parameter setting is $\sigma_q^2 = 1000$. Figs. 5, 6, and 7 display the simulated and theoretical tracking EMSE vs. μ for different values of σ_b^2, σ_h^2, and M, where $c = 4$ for Figs. 5 and 6, $c = 7$ for Fig. 7. The minimum EMSE and the optimal step size μ_o are also shown.

In Fig. 5, an increase of σ_h^2 leads to higher minimum EMSE and lower optimal μ_o for the given σ_b^2. As can be seen in Fig. 6, the optimal μ_o and minimum EMSE decrease as σ_h^2 decreases for a given σ_b^2. From Fig. 7, the minimum EMSE does not vary much with the projection-order M for given σ_b^2 and σ_h^2. The optimal step size decreases monotonically with increasing the projection order M. The high accuracy of the theoretical expressions can be clearly verified from these simulation results over a range of step-sizes, σ_b^2, σ_h^2, and M values.

D. AEC Application

Herein, the convergence of SSA is evaluated for AEC application. In AEC, an AF is to identify acoustic echo path between microphone and loudspeaker (see Fig. 8, which shows the AEC block diagram). The filter output signal is subtracted from the microphone signal for echo cancellation. To show the superiority of devised SSA against known algorithms, three

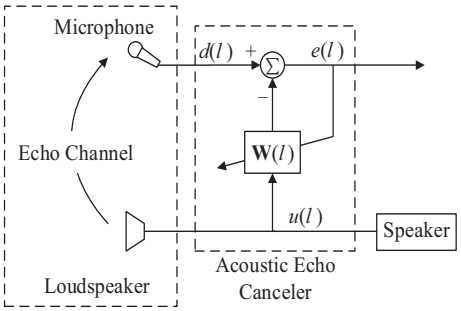

Fig. 8: Block-diagram of an AEC system.

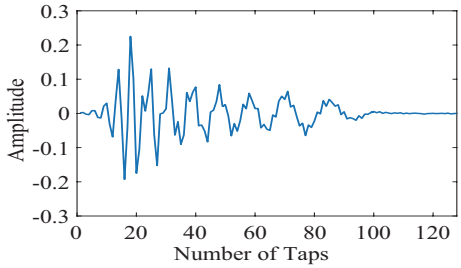

Fig. 9: Echo CIR with 128 taps.

types of input signal are considered in the simulations: zero-mean white Gaussian signal with unit variance, AR signal, and an authentic speech-signal sampled at 8 kHz shown in Fig. 10. The unknown channel is the echo-channel given by the ITU-T G.168 with 128 taps [33] which is shown in Fig. 9. M for all algorithms is 4. The other parameters are set as $\mathrm{SIR} = -30\mathrm{dB}$ and $\mathrm{SNR} = 30\mathrm{dB}$. The regularized parameters for APS, MIPS-APS, and APV are 10^{-6}. The step size μ and various parameters are given in figures and they are selected to obtain same NMSD or initial convergence rate.

Figs. 11 and 12 show the performance curves for the algorithms with $P = 0.001$ and $P = 0.1$, respectively. Figures 11 and 12 show that the APS, MIPS-APS, APV, and SSA algorithms are robust in impulsive environments with different values of the occurrence probability, except the AP algorithm, and the SSA algorithm always works better than mentioned algorithms.

VII. Conclusions

This article proposes a squared sine adaptive (SSA) algorithm by using the squared sine function on the error vector to create a new cost-function. The SSA shows robustness in the impulsive environment and speed-ups convergences for colored inputing signals. The theoretical models for predicting the mean weight behavior, transient EMSE behavior, and tracking behavior are developed and verified using simulations. Furthermore, the optimal step-size and minimum EMSE are

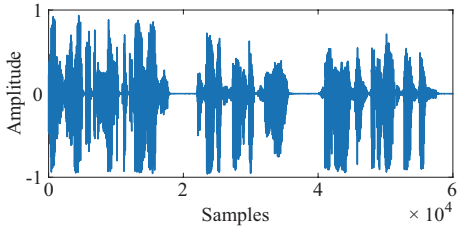

Fig. 10: Speech input signal for AEC Application.

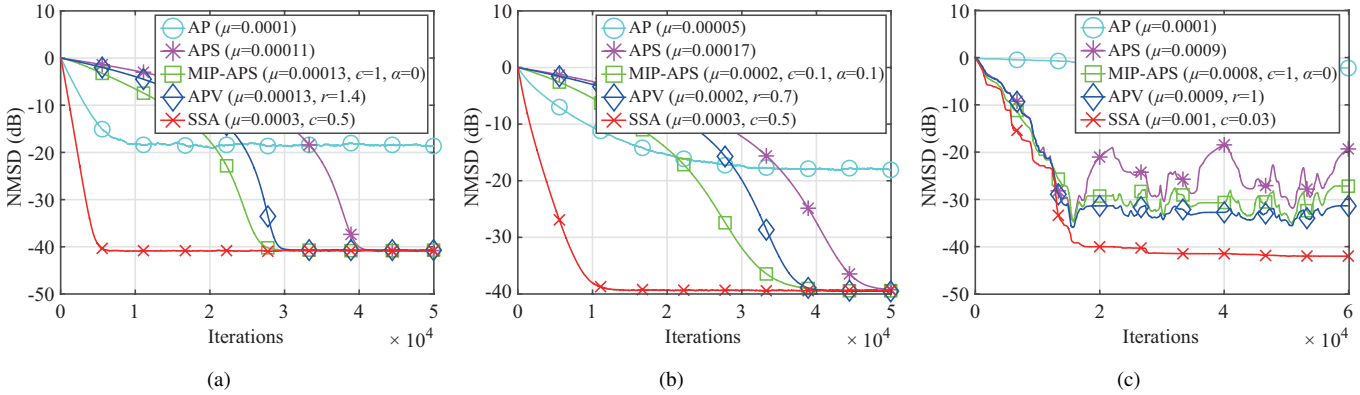

Fig. 11: Convergence of AP, APS, MIPS-APS, APV, and SSA with different input signals and $P = 0.001$. (a) WGN signal; (b) AR signal; (c) Speech signal.

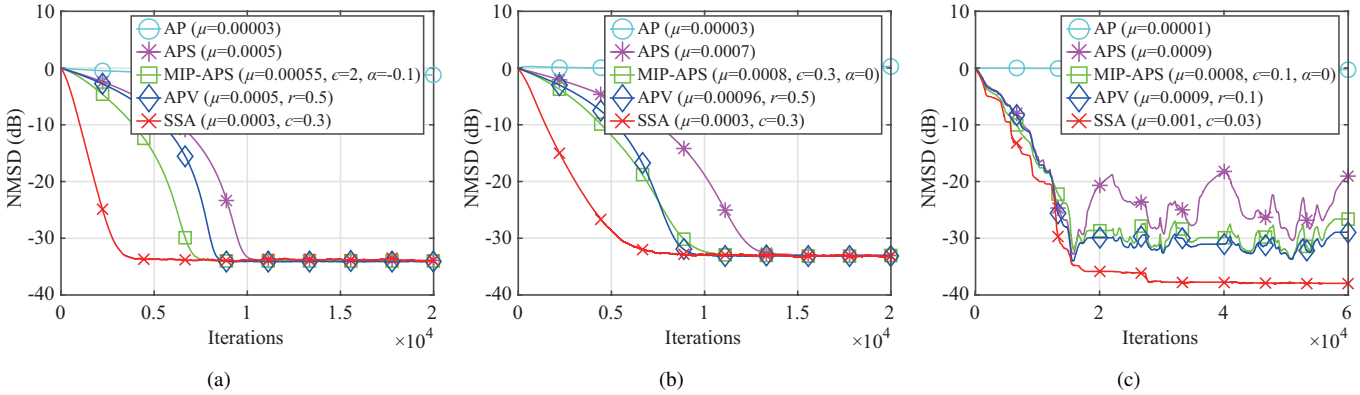

Fig. 12: Convergence of AP, APS, MIPS-APS, APV, and SSA with different input signals and $P = 0.1$. (a) WGN signal; (b) AR signal; (c) Speech signal.

provided for time-varying systems. Also, we investigated the computation complexity of the algorithm and showed that the SSA algorithm is simpler than the other algorithms. Experimental results demonstrate that theoretical prediction matches well with experimental results under different occurrence probabilities, projection-orders, step sizes, σ_b^2, and σ_h^2 values. The experimental results confirm the superiority of devised SSA algorithm against known AP-like AF algorithms.

REFERENCES

[1] S. S. Haykin, *Adaptive Filter Theory*, 4th ed., Englewood Cliffs, NJ, USA: Prentice-Hall, 2002

[2] A. H. Sayed, *Fundamentals of Adaptive Filtering*. New York, NY, USA: Wiley, 2003.

[3] L. Shi, H. Zhao, and Y. Zakharov, "Performance analysis of shrinkage linear complex-valued LMS algorithm," *IEEE Signal Process. Lett.*, vol. 26, no. 8, pp. 1202-1206, Aug. 2019.

[4] H. Huang and J. Lee, "A new variable step-size NLMS algorithm and its performance analysis," *IEEE Trans. Signal Process.*, vol. 60, no. 4, pp. 2055-2060, Apr. 2012.

[5] Y. Li, Y. Wang, and T. Jiang, "Norm-adaption penalized least mean square/fourth algorithm for sparse channel estimation," *Signal Process.*, vol. 128, no. 2016, pp. 243-251, Apr. 2016.

[6] Y. Li, Y. Wang, and T. Jiang, "Sparse-aware set-membership NLMS algorithms and their application for sparse channel estimation and echo cancelation," *AEU-Int. J.Electron. Commu.*, vol. 70, no. 7, pp. 895-902, Jul. 2016.

[7] L. Shi, H. Zhao, Y. Zakharov, B. Chen and Y. Yang, "Variable step-size widely linear complex-valued affine projection algorithm and performance analys," *IEEE Trans. Signal Process.*, vol. 68, pp. 5940-5953, Oct. 2020.

[8] M. Rupp, "A family of adaptive filter algorithms with decorrelation properties," *IEEE Trans. Signal Process.*, vol. 46, no. 3, pp. 771-775, Mar. 1998.

[9] H. C. Shin and A. H. Sayed, "Mean-square performance of a family of affine projection algorithms," *IEEE Trans. Signal Process.*, vol. 52, no. 1, pp. 90-102, Jan. 2004.

[10] Z. Zheng, Z. Liu, and Y. Dong, "Steady-state and tracking analyses of the improved proportionate affine projection algorithm," *IEEE Trans. Circuits Syst. II, Express Briefs*, vol. 65, no. 11, pp. 1793-1797, Nov. 2018.

[11] S. J. Ban, C. W. Lee, and S. W. Kim, "Adaptive regularization parameter for pseudo affine projection algorithm," *IEEE Signal Process. Lett.*, vol. 16, no. 5, pp. 382-385, May 2009.

[12] W. A. Martins, M. V. S. Lima, P. S. R. Diniz, and T. N. Ferreira, "Optimal constraint vectors for set-membership affine projection algorithms," *Signal Process.*, vol. 134, pp. 285-294, Jan. 2017.

[13] T. Shao, Y. R. Zheng, and J. Benesty, "An affine projection sign algorithm robust against impulsive interferences," *IEEE Signal Process. Lett.*, vol. 17, no. 4, pp. 327-330, Apr. 2010.

[14] F. Huang , J. Zhang, and S. Zhang, "Affine projection Versoria algorithm for robust adaptive echo cancellation in hands-free voice communications," *IEEE Trans. Veh. Technol.*, vol. 67, no. 12, pp. 11924-11935, Dec. 2018.

[15] F. Albu, H.K. Kwan, "Memory improved proportionate affine projection sign algorithm," *Electron. Lett.*, vol. 48, no. 20, pp. 1279-1281, Sep. 2012.

[16] M. Z. A. Bhotto, M. O. Ahmad, and M. N. S. Swamy, "Robust shrinkage affine-projection sign adaptive-filtering algorithms for impulsive noise environments," *IEEE Trans. Signal Process.*, vol. 62, no. 13, pp. 3349-3359, Jul. 2014.

[17] A. Singh and J. C. Principe, "Using correntropy as a cost function in linear adaptive filters," *in Proc. Int. Joint Conf. Neural Netw.*, 2009, pp. 2950-2955.

[18] W. Shi, Y. Li, and Y. Wang, "Noise-free maximum correntropy criterion

algorithm in non-Gaussian environment," *IEEE Trans. Circuits Syst. II, Express Briefs*, vol. 67, no. 10, pp. 2224-2228, Oct. 2020.

[19] T. Ogunfunmi and T. Paul, "The quarternion maximum correntropy algorithm," *IEEE Trans. Circuits Syst. II, Express Briefs*, vol. 62, no. 6, pp. 598-602, Feb. 2015.

[20] B. Chen, L. Xing, H. Zhao, N. Zheng, and J. C. Principe, "Generalized correntropy for robust adaptive filtering," *IEEE Trans. Signal Process.*, vol. 64, no. 13, pp. 3376-3387, Jul. 2016.

[21] Y. Li, Z. Jiang, W. Shi, X. Han, and B. Chen, "Blocked maximum correntropy criterion algorithm for cluster-sparse system identifications," *IEEE Trans. Circuits Syst. II, Express Briefs*, vol. 66, no. 11, pp. 1915-1919, Nov. 2019.

[22] F. Huang, J. Zhang, and S. Zhang, "Adaptive filtering under a variable kernel width maximum correntropy criterion," *IEEE Trans. Circuits Syst. II, Express Briefs*, vol. 64, no. 10, pp. 1247-1251, Oct. 2017.

[23] W. Shi, Y. Li, and B. Chen, "A separable maximum correntropy adaptive algorithm," *IEEE Trans. Circuits Syst. II, Express Briefs*, vol. 67, no. 11, pp. 2797-2801, Nov. 2020.

[24] J. Zhao, H. Zhang, and J. A. Zhang, "Generalized maximum correntropy algorithm with affine projection for robust filtering under impulsive-noise environments," *Signal Processing*, vol. 172, pp. 1-6, ID:107524, Jul. 2020.

[25] D. F. Andrews, "A robust method for multiple linear regression," *Technometrics*, vol. 16, no. 4, pp. 523-531, Apr. 1974.

[26] M. J. Black and A. Rangarajan "On the unification of line processes, outlier rejection, and robust statistics with applications in early vision," *Int. J. Comput. Vision*, vol. 19, no. 4, pp. 57-91, 1996.

[27] X. Huang, Y. Li, Y. Zakharov, Y. Li, and B. Chen, "Affine-projection lorentzian algorithm for vehicle hands-free echo cancellation," *IEEE Trans. Veh. Technol.*, vol. 70, no. 3, pp. 2561-2575, Feb. 2021.

[28] T. Y. Al-Naffouri, and A. H. Sayed, "Transient analysis of data-normalized adaptive filters," *IEEE Trans. Signal Process.*, vol.51, no.3, pp.639-652, 2003.

[29] A. Carini, and G. L. Sicuranza, "Transient and steady-state analysis of filtered-x affine projection algorithms," *IEEE Trans. Signal Process.*, vol.54, no.2, pp.665-678, 2006

[30] Y. Peng, S. Zhang, J. Zhang and W. Zheng "Combined-sample multiband-structured subband filtering algorithms," *IEEE Trans. Audio, Speech, Lang. Process.,*, vol. 30, pp. 1083-1092, Mar. 2022.

[31] C. Qiu, G. Qian and S. Wang, "Widely linear maximum complex correntropy criterion affine projection algorithm and its performance analysis," *IEEE Trans. Signal Process.*, vol. 70, pp. 3540-3550, June 2022.

[32] J. Chen, C. Richard, J. C. M. Bermudez, and P. Honeine, "Nonnegative least-mean-square algorithm," *IEEE Trans. Signal Process.*, vol. 59, no. 11, pp. 5225-5235, Nov. 2011.

[33] *ITU-T Recommendation G.168, Digital Network Echo Cancellers*, Int. Telecommun. Union, Geneva, Switzerland, 2007.